ELSEVIER

Phosphorus sulfide as a functional material for sodium-ion batteries

Tatiana L. Kulova,[a] Alexander M. Skundin,*[a] Dmitry Yu. Gryzlov,[a]
Yulia O. Kudryashova[a,b] and Andrey A. Chekannikov[c]

[a] *A. N. Frumkin Institute of Physical Chemistry and Electrochemistry, Russian Academy of Sciences, 119071
Moscow, Russian Federation. Fax: +7 495 952 5308; e-mail: askundin@mail.ru*
[b] *National Research University 'MPEI', 111250 Moscow, Russian Federation*
[c] *Skolkovo Institute of Science and Technology, 143025 Moscow, Russian Federation*

A carbon-supported composite with the formula P_4S_3 was synthesized and a possibility of reversible sodium insertion into this material was explored. The reversible capacity of the material was 885 mAh g^{-1} at a current intensity of 20 mA g^{-1}, and the capacity loss in 100 cycles did not exceed 10%.

Charge
$$P_4S_3 + 18Na \rightleftarrows 3Na_2S + 4Na_3P$$
Discharge

Q_{disch} = 885 mAh g^{-1}

P_4S_3 Na
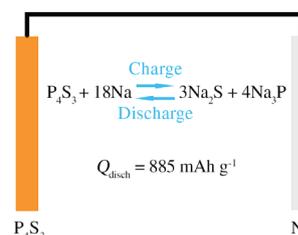
Sodium-ion batteries are promising rechargeable power sources since their specific theoretical characteristics are insignificantly inferior to those of lithium-ion batteries, while they are much less expensive. Currently, various materials based on carbon, individual metals and alloys, metal oxides, phosphorus, *etc.*, can be used in the negative electrodes of sodium-ion batteries.[1,2] Phosphorus materials (elemental phosphorus and phosphides)[3–8] possess some advantages over other functional materials, and they are of interest because the reversible insertion of sodium into phosphorus and phosphides proceeds *via* a multielectronic reaction, in which 18 electrons can participate.[5] Various metal phosphides have been reported as potential negative electrodes for sodium-ion and lithium-ion batteries, while the selenium phosphides Se_3P_4 and Se_4P_4 demonstrated promising characteristics.[9,10] Similarly to phosphorus selenides, phosphorus sulfides may serve as negative electrodes in sodium-ion batteries, and the aim of this work was to evaluate the applicability of phosphorus sulfide as a functional material for the negative electrode of a sodium-ion battery.

Phosphorus sulfide on a carbon support was synthesized from red phosphorus and sulfur, which were preliminary dried in an atmosphere of argon over P_2O_5. Carbon black Ketjechen Black-300 (KB-300) was dried *in vacuo* at 200 °C for 8 h. Stoichiometric amounts of red phosphorus (P) and sulfur (S) were carefully ground in an agate mortar, and 30 wt% KB-300 carbon black was added to the P–S mixture. The resulting mixture was thoroughly ground again in the agate mortar and placed in a sealed stainless steel capsule, which was heated in a tubular oven at 470 °C for 2 h. The operations were carried out in an airtight glovebox filled with argon. Once the capsule was cooled down to room temperature, it was opened in air, and an active mass for electrodes was prepared from the resulting composite (P-S-KB-300). For this purpose, composite P-S-KB-300 (90 wt%) was mixed with a cooled solution of carboxymethyl cellulose (10 wt%) in a mixture of distilled water and ethanol. The resulting mixture was homogenized using an ultrasonic disperser for 1 min. The resulting active mass was distributed onto stainless steel mesh current collectors using a

spatula and vacuum dried at 60 °C for 8 h to remove water traces. The active substance amount on the current collector was 5–7 mg cm^{-2}. The electrodes were tested in gas-tight three-electrode cells with sodium foil used as both reference and counter electrodes. A 1 M solution of $NaPF_6$ in a mixture of ethylene carbonate–diethyl carbonate–dimethyl carbonate (1 : 1 : 1, v/v) was used as an electrolyte. The water content of the electrolyte was no higher than 15 ppm, as measured by coulometric Fisher titration.

The results of scanning electron microscopy (SEM)[†] and electron-dispersive analysis showed that phosphorus and sulfur were evenly distributed on the KB-300 surface, and the synthesized phosphorus sulfide corresponded to the formula P_4S_3 (Figure 1).
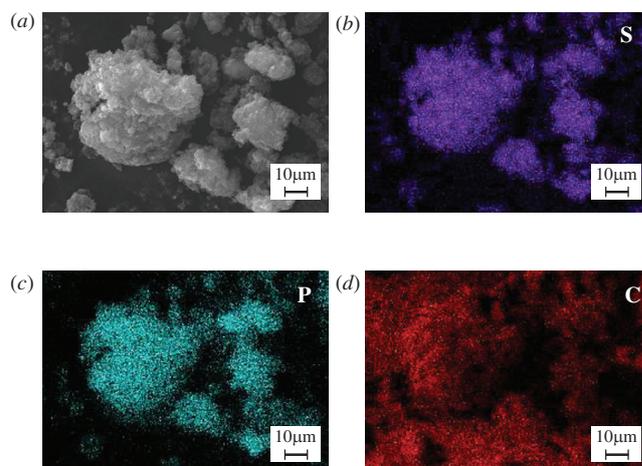
Figure 1 (*a*) SEM image of the composite P_4S_3 with carbon and distribution maps of the elements: (*b*) P, (*c*) S, and (*d*) C.

[†] A JEOL JSM 6490 LV scanning electron microscope was used to observe the morphology and particle size.
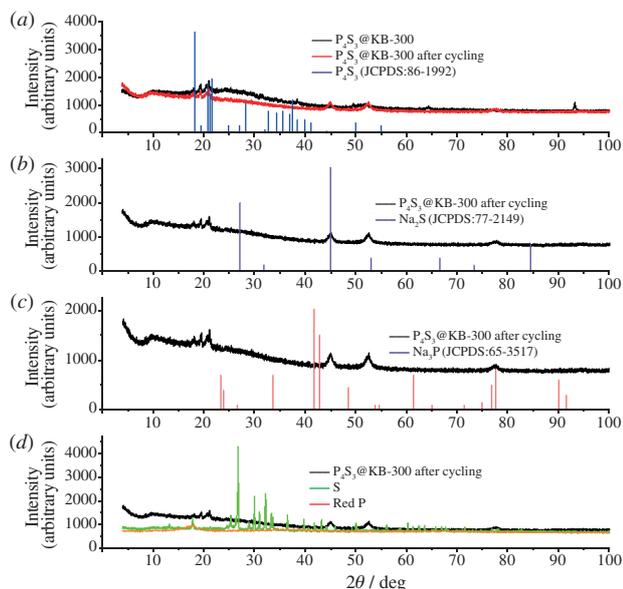
Figure 2 XRD spectra of (*a*) P-S-KB-300 composite (freshly prepared and after cycling), (*b*) P-S-KB-300 after cycling compared with a reference standard of Na_2S, (*c*) P-S-KB-300 after cycling compared with a reference standard of Na_3P, and (*d*) P-S-KB-300 after cycling compared with the spectra of elemental sulfur and phosphorus.

The XRD analysis‡ of a freshly prepared electrode indicated the presence of P_4S_3 and the absence of elemental sulfur and phosphorus [Figure 2(*a*)].

Electrochemical investigations conducted in the galvanostatic mode§ showed that the reversible insertion of sodium into the synthesized composite proceeded at potentials from 0.01 to 3 V. Figure 3 shows galvanostatic charge and discharge curves recorded at a current of 20 mA g⁻¹ for the first 20 cycles and 100 mA g⁻¹ for the first 100 cycles.

According to Figure 3, a charge at the first cathode polarization exceeds significantly that of the subsequent cycles. This effect is associated with the well-known process of reduction of the electrolyte components (mainly solvent) with the formation of insoluble products deposited as a thin passive film (a so-called solid electrolyte interphase, SEI) on the electrode surface. The SEI possesses ionic conductivity and does not hinder the transport of sodium ions, but it protects the electrode surface from a contact with the electrolyte, which prevents (or at least, severely inhibits) its further reduction.[11,12] The coulombic efficiency for the first cycle was 54%, while it increased to almost 90% during further cycling.
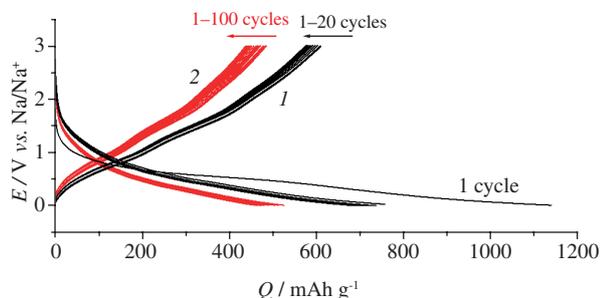

Figure 3 Charge (cathodic) and discharge (anodic) curves recorded using an electrode of the composite of phosphorus sulfide with carbon at a current of (*1*) 20 mA g⁻¹ (black curves) and (*2*) 100 mA g⁻¹ (red curves).

Two plateaus at the potentials of 0.75 and 1.5 V can be distinguished on the anodic part of curve corresponding to the extraction of sodium, which indicates stepwise nature of the anodic process.

Similarly to the insertion of sodium into phosphorus selenide,[10] such a process for phosphorus sulfide can be described by the following mechanism. At the first cathode polarization, phosphorus sulfide irreversibly decomposes to form sodium sulfide and phosphide:

$$P_4S_3 + 18Na^+ + 18e^- \rightarrow 3Na_2S + 4Na_3P. \qquad (1)$$
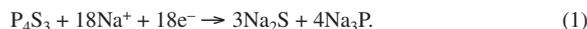
The reverse process proceeds *via* the two simultaneous reactions:

$$3Na_2S \leftrightarrow 3S + 6Na^+ + 6e^-, \qquad (2)$$

$$4Na_3P \leftrightarrow 4P + 12Na^+ + 12e^-. \qquad (3)$$

A theoretical specific capacity for sodium insertion into P_4S_3 calculated according to equation (1) is 2192 mAh g⁻¹. However, the reversible capacity for sodium insertion into the composite was 620 mAh g⁻¹ (on a composite basis) or 885 mAh g⁻¹ (on a phosphorus sulfide basis). Such a difference in the theoretical and practical capacities allowed us to also assume the following alternative reaction scheme of a reversible process without the formation of sulfur and phosphorus in elemental states:

$$P_4S_3 + 18Na^+ + 18e^- \leftrightarrow 3Na_2S + 4Na_3P. \qquad (4)$$

Indeed, the XRD study of the electrode after cycling revealed no signs of sulfur and phosphorus [Figure 2(*d*)]. At the same time, this study revealed some amounts of Na_3P and Na_2S [Figures 2(*b*), 2(*c*)]. This can be due to the passivation of a portion of the product, which can explain a diminished capacity obtained in this work.

Prolonged cycling at a current density of 100 mA g⁻¹ showed that the capacity loss per 100 cycles did not exceed 10%, which indicates the absence of strong morphological changes in the synthesized composite and demonstrates prospects for its applications in the negative electrodes of sodium-ion batteries.

References

1 A. M. Skundin, T. L. Kulova and A. B. Yaroslavtsev, *Russ. J. Electrochem.*, 2018, **54**, 113 (*Elektrokhimiya*, 2018, **54**, 131).
2 T. L. Kulova and A. M. Skundin, *Russ. Chem. Bull., Int. Ed.*, 2017, **66**, 1329 (*Izv. Akad. Nauk, Ser. Khim.*, 2017, 1329).
3 Y. Fu, Q. Wei, G. Zhang and S. Sun, *Adv. Energy Mater.*, 2018, **8**, 1702849.
4 D. Zhao, L. Zhang, C. Fu, J. Zhang and C. Niu, *Nano Research*, 2019, **12**, 1.
5 W. Liu, H. Zhi and X. Yu, *Energy Storage Mater*, 2019, **16**, 290.
6 P. Mei, J. Kim, N. A. Kumar, M. Pramanik, N. Kobayashi, Y. Sugahara and Y. Yamauchi, *Joule*, 2018, **2**, 2289.
7 X. Han, J. Han, C. Liu and J. Sun, *Adv. Funct. Mater.*, 2018, **28**, 1803471.
8 Z. Li, and H. Zhao, *J. Mater. Chem. A*, 2018, **6**, 24013.
9 Y. Cao, M. K. Majeed, Y. Li, G. Ma, Z. Feng, X. Ma and W. Ma, *J. Alloys Compd.*, 2019, **775**, 1286.
10 Y. Lu, P. Zhou, K. Lei, Q. Zhao, Z. Tao and J. Chen, *Adv. Energy Mater.*, 2017, **7**, 1601973.
11 N. Yabuuchi, Y. Matsuura, T. Ishikawa, S. Kuze, J.-Y. Son, Y.-T. Cui, H. Oji and S. Komaba, *ChemElectroChem*, 2014, **1**, 580.
12 P. Thomas and D. Billaud, *Electrochim. Acta*, 2002, **47**, 3303.